Analysis of Lithospheric Stresses Using Satellite Gravimetry: Hypotheses and Applications to North Atlantic

Alexander Minakov & Sergei Medvedev,
Centre for Earth Evolution and Dynamics, University of Oslo (alexander.minakov@geo.uio.no)

AGU New Orleans 11-15 Dec. 2017
DI23A-0424
Tuesday, 12 December 2017 13:40 - 18:00 New Orleans Ernest N. Morial Convention Center - Poster Hall D-F

1. MOTIVATION

A major source of lithospheric stresses is believed to be in variations of surface topography and lithospheric density. The traditional approach to stress estimation is based on direct calculations of the Gravitational Potential Energy (GPE), the depth integrated density moment of the lithosphere column and upper mantle. GPE is highly sensitive to density structure which, however, is often poorly constrained. Density structure of the lithosphere may be refined using methods of gravity modeling. However, the resulted density models suffer from non-uniqueness of the inverse problem. An alternative approach is to directly estimate lithospheric stresses (depth integrated) from satellite gravimetry data.

Satellite gravity gradient measurements by the ESA GOCE mission ensures a wealth of data for mapping lithospheric stresses if a link between data and stresses or GPE can be established theoretically. Following (Camelbeeck et al., 2013), we adopt the method (1) that constrains lithospheric stresses by direct utilization of the gravity gradient tensor. For comparison, we use more traditional methods as well: (2) the filtered geoid approach (e.g., Chase et al., 2002; Coblentz et al., 2015), and (3) the direct thin-sheet approximation based on depth integration of density moment (e.g., Medvedev, 2016). Whereas the last two approaches (2)-(3) calculate GPE and utilize a computationally expensive finite element mechanical modeling to calculate stresses, the approach (1) uses a much simpler numerical treatment but requires simplifying assumptions that yet to be tested. We applied all methods to the North Atlantic region where reliable additional constraints are available and tested results against the World Stress Map.

2. LITHOSPHERIC STRESSES AND GRADIENTS OF GRAVITATIONAL POTENTIAL - CONCEPTUAL MODEL

Local lithospheric stress perturbation hypothesis

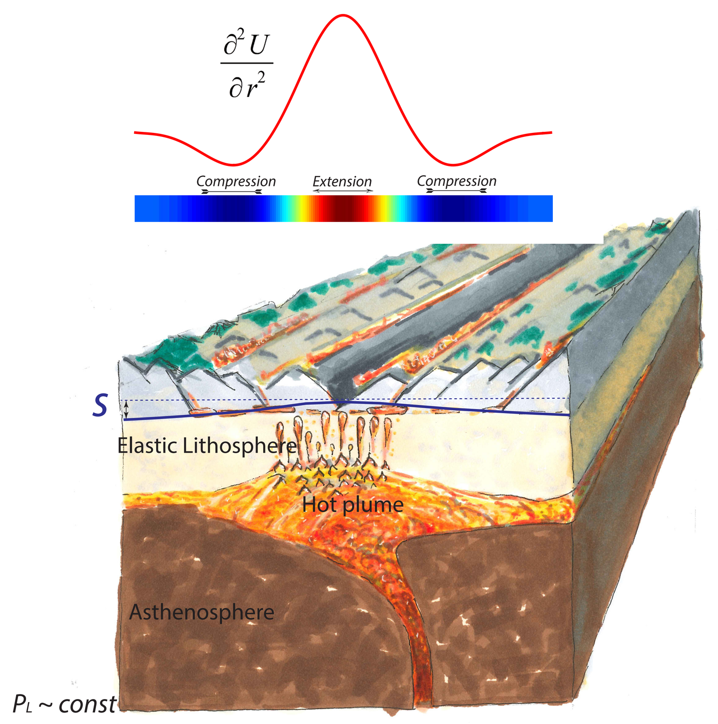

Isostatic topography due to idealized temperature perturbation in upper mantle

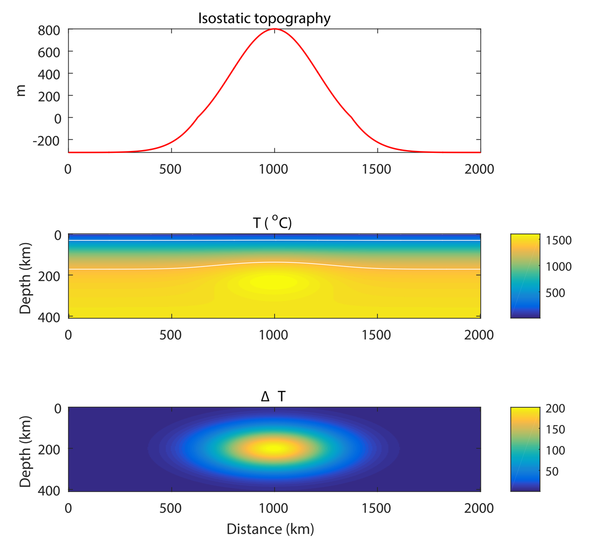

Gravity response due to locally compensated mantle thermal density anomaly

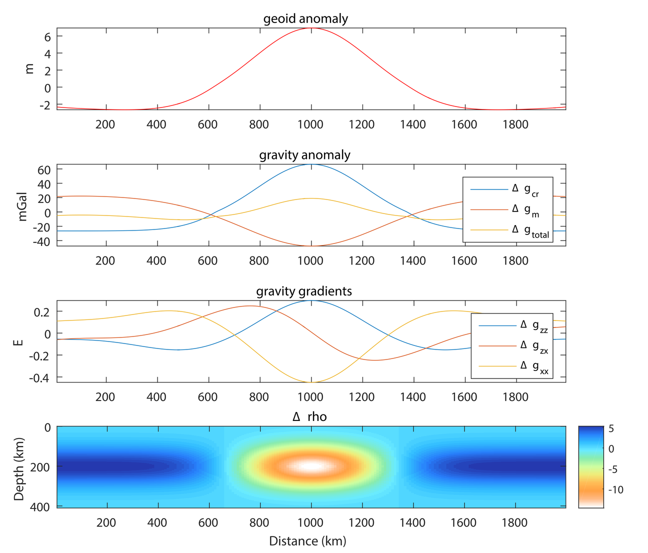

$$quantity^{\text{Lagrangian}} = quantity^{\text{Eulerian}} + \mathbf{s}\cdot\nabla quantity$$

$$\mathbf{r}(\mathbf{x},t) = \mathbf{x} + \mathbf{s}(\mathbf{x},t) \qquad D_t = \partial_t + \mathbf{u}^{E}\cdot\nabla_{\mathbf{r}} \quad \text{Material derivative}$$

Linearized form of the Lagrangian momentum equation:

$$\nabla_{\mathbf{x}}\cdot\mathbf{T}^{\text{PK1}} = -\rho^0\mathbf{g}^{\text{L1}} = -\rho^0\mathbf{g}^{\text{E1}} - \rho^0\mathbf{s}\cdot\nabla\mathbf{g}^0 = \rho^0\nabla\phi^{\text{E1}} + \rho^0\mathbf{s}\cdot\nabla\nabla\phi^0$$

$$\mathbf{g}^{\text{L}} = \mathbf{g}^0 + \mathbf{g}^{\text{L1}}$$ for incremental stress perturbation (away from static stress equlibrium)

(Dahlen & Tromp 1998)

3. DATA AND CONSTRAINTS

3.1 NORTH ATLANTIC REGION AND ICELAND HOTSPOT

The lithospheric structure of the North Atlantic is controlled by ~56 Ma seafloor spreading and Iceland Hotspot (peak of most recent activity at 23-7 Ma).

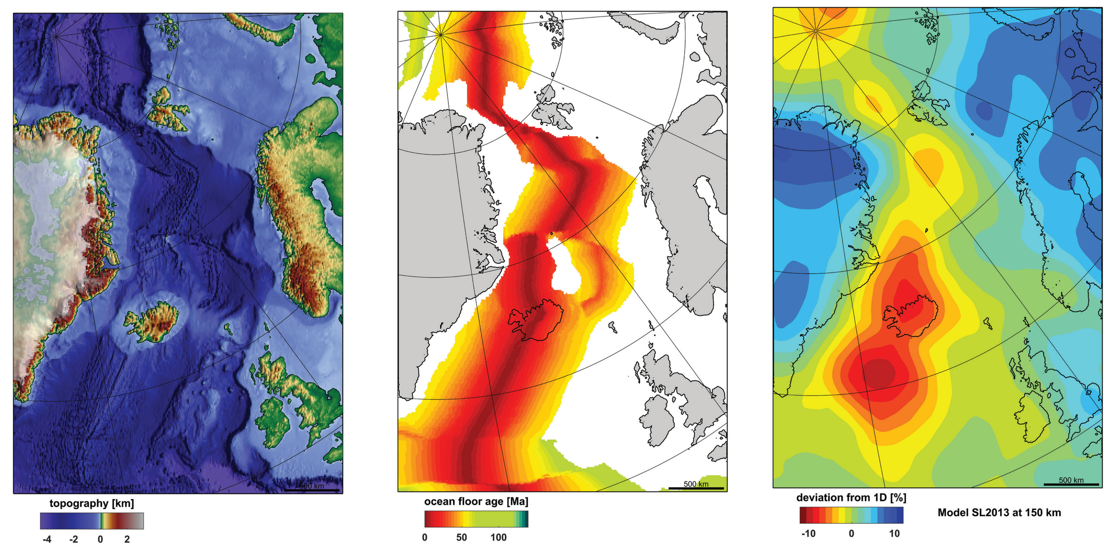

Topography and bathymetry of the area ETOPO-1 (Amante and Eakins, 2009). Oceanic crustal age (Gaina et al. 2017) Shear-wave velcoity model based on results of seismic surface wave tomography. Slice at 150 km (Schaeffer & Lebedev 2013)

3.2 GOCE SATELLITE GRAVITY GRADIENT DATA

The gravitational gradients (Bouman et al. 2016) recently obtained by the ESA's mission GOCE (Gravity field and steady-state Ocean Circulation Explorer) can be used globally to obtain density models of the lithosphere and upper mantle. Unlike geoid, gravity gradients are less sensitive to deep mantle structures.

Gradients in local north-oriented reference frame

$$\mathbf{T} = [T_{WW}, T_{WN}, T_{WR}, T_{NN}, T_{NR}, T_{RR}]$$

Laplace equation:

$$\nabla^2 U = T_{WW} + T_{NN} + T_{RR} = 0$$

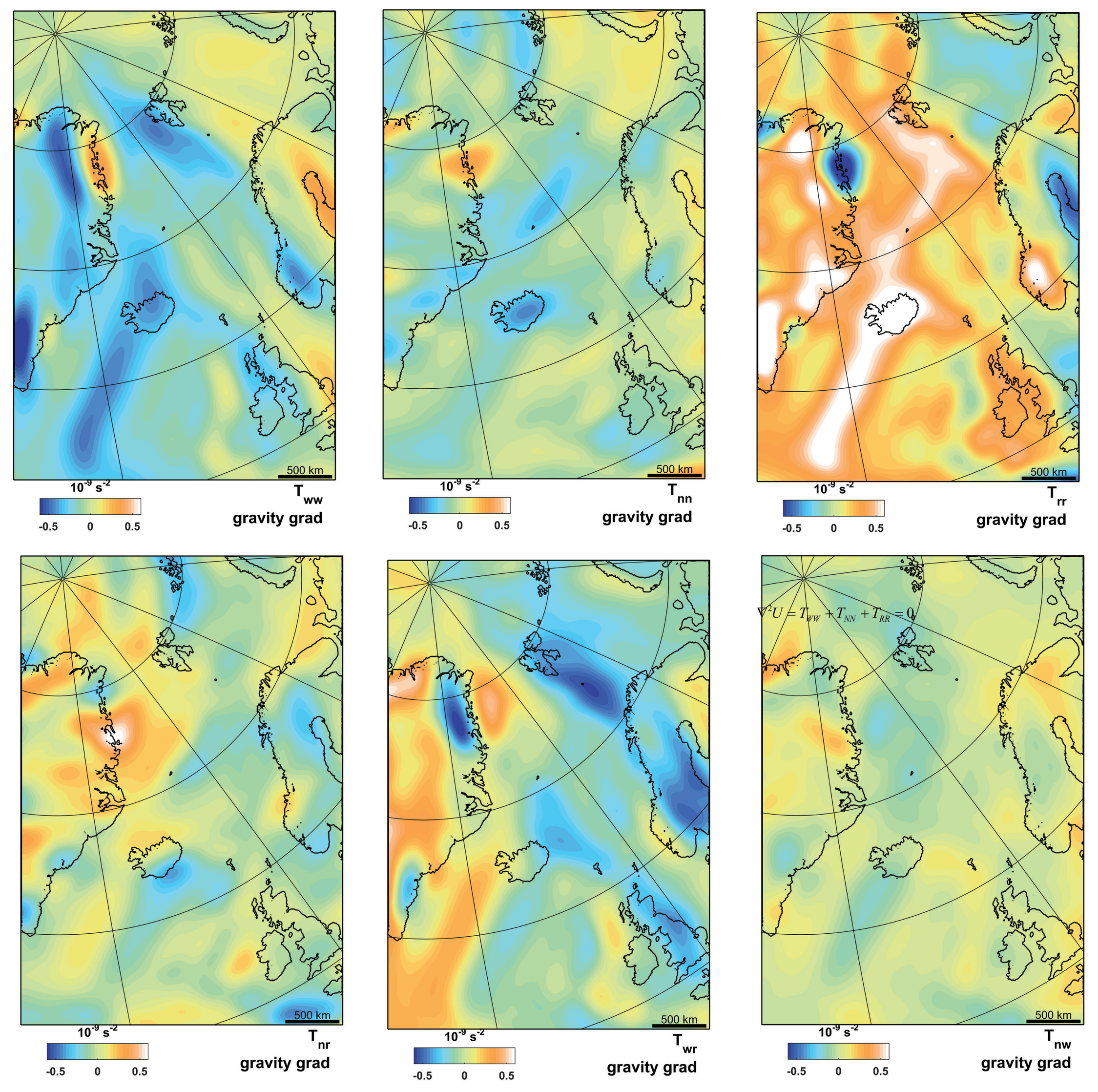

4. METHOD 1. STRESSES PREDICTED USING SATELLITE GRAVITY GRADIENT TENSOR

The method of direct estimation of local (depth-integrated) lithospheric stress perturbation from gravity gradient tensor generally follows Camelbeeck et al. 2013. The method assumes that local perturbation of depth integrated horizontal stresses is proportional to divergence of geoid gradient.

$$\nabla\cdot\mathbf{F} = -2.3\times10^{11}\left(T_{XX}+T_{YY}\right)$$ or using 2D principal values $$-2.3\times10^{11}\left(T_1^s+T_2^s\right)$$

4.1 EIGENVALUES OF GRAVITY GRADIENT TENSOR

Principal values from eigendecomposition of **T** $\quad (\mathbf{T}-\lambda_i\mathbf{I})\mathbf{v} = 0 \qquad T_1 + T_2 + T_3 = 0$

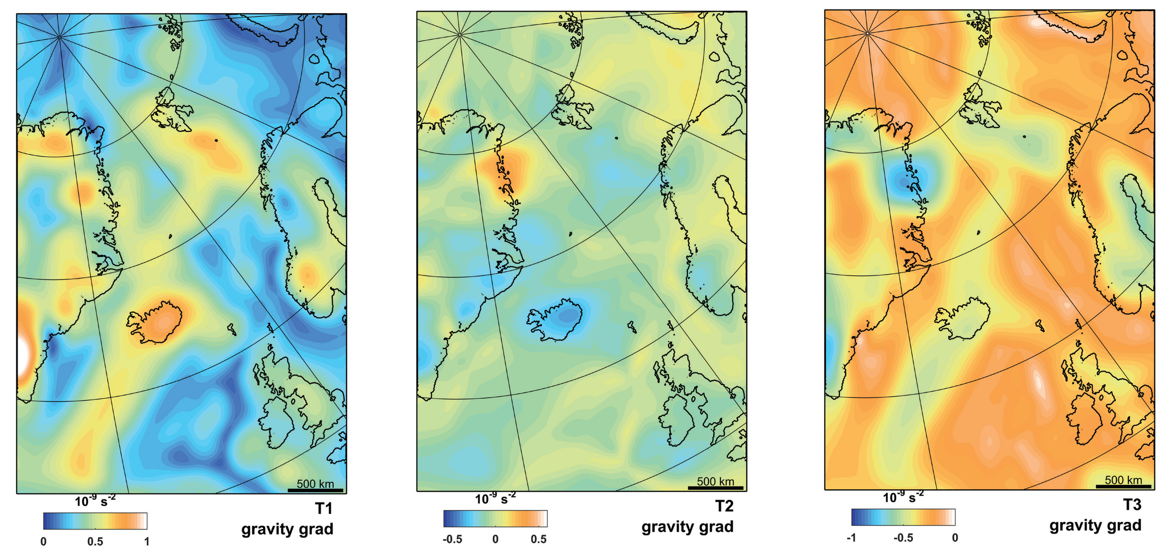

4.2 PREDICTED INTEGRATED LITHOSPHERIC STRESSES

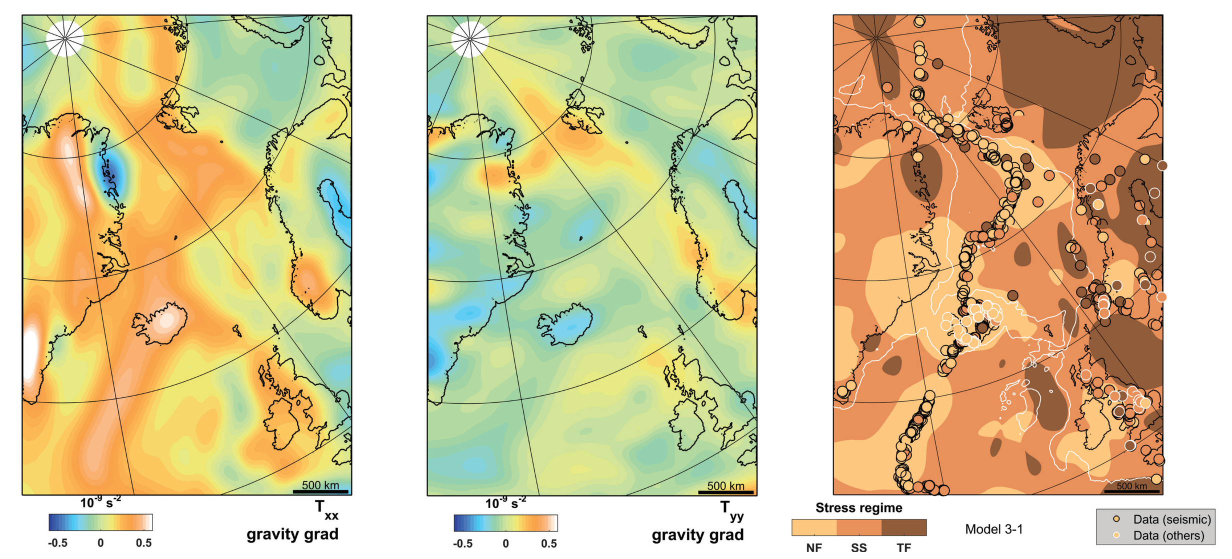

Horizontal gravity gradients transformed to local coordinates **Stress regime**

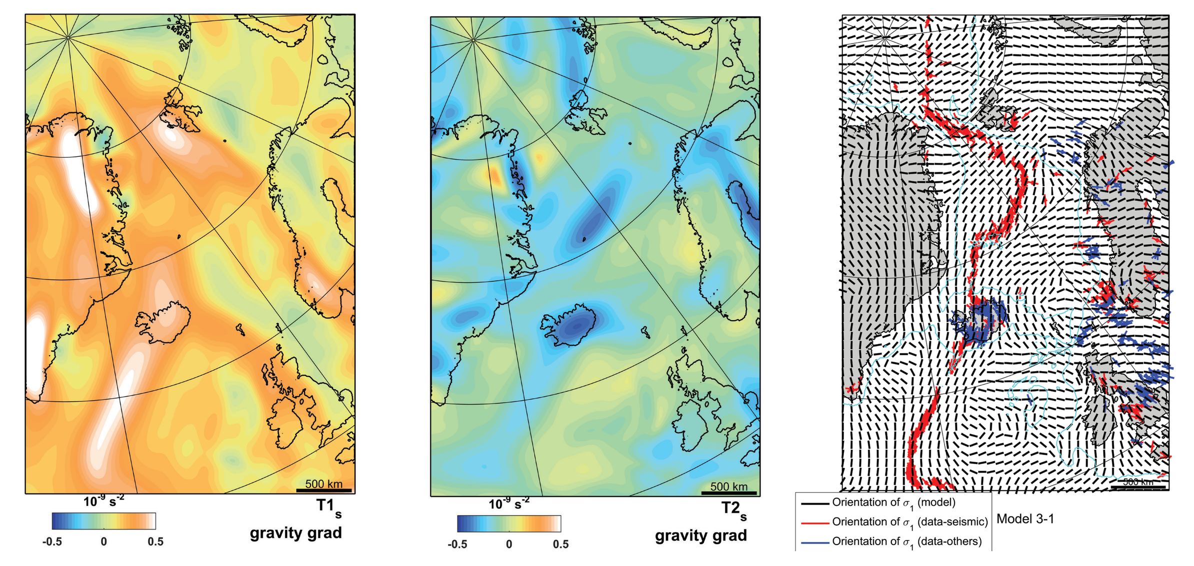

Eigenvalues of horizontal 2D gravity gradient tensor **Max. principal horizontal stress**

The quality of the modelled stress regime was estimated using the tectonic stress regime index (Delvaux et al., 1997).

5. THIN-SHEET NUMERICAL MECHANICAL MODELING

5.1 METHOD 2. GPE BASED ON FILTERED GEIOD ANOMALIES

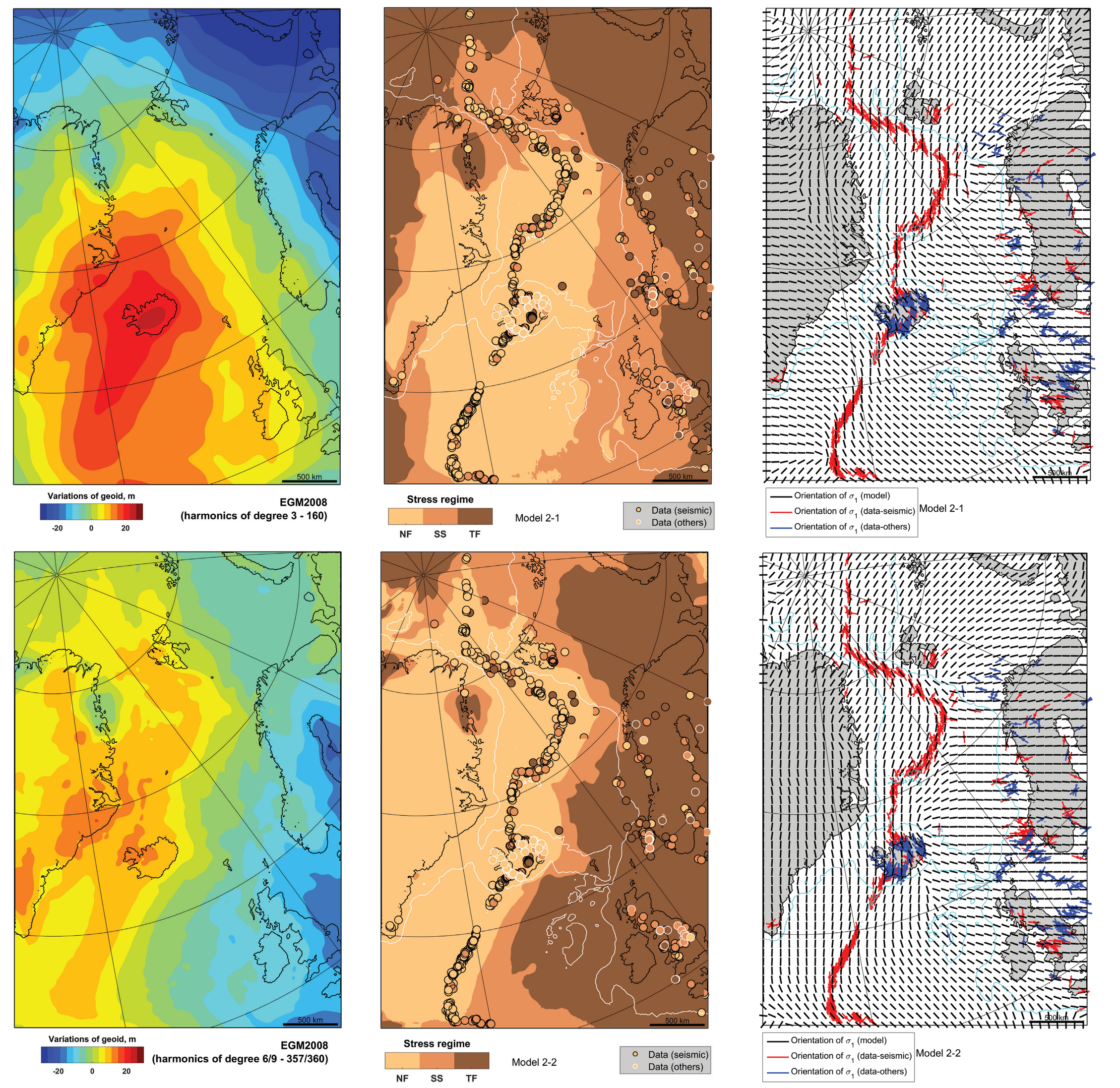

ProShell approach (Medvedev 2016) includes in-plane and bending deformation and is able to consider the complicated geometry of the plate, such as curvature of the lithospheric shell. The numerical model was constrained in several steps. We calculate GPE using filtered geoid anomalies (Method 2; 5.1) and a density model for lithosphere and upper mantle (Method 3; 5.2). We then consider balance of stresses and moments in a single element of the finite-element mesh. In the local system of coordinates attached to this element (with axes X and Y defining the horizon of the local plate), the system of equations are derived from the integration of the 3D momentum:

$$\frac{\partial\bar{\sigma}_x}{\partial x} + \frac{\partial\bar{\sigma}_{xy}}{\partial y} + F_x = \frac{\partial\Pi}{\partial x}$$

$$\frac{\partial\bar{\sigma}_{xy}}{\partial x} + \frac{\partial\bar{\sigma}_y}{\partial y} + F_y = \frac{\partial\Pi}{\partial y}$$

$$\frac{\partial M_x}{\partial x} + \frac{\partial M_{xy}}{\partial y} + Q_x = 0 \qquad \frac{\partial Q_x}{\partial x} + \frac{\partial Q_y}{\partial y} + \Delta p = 0$$

$$\frac{\partial M_{xy}}{\partial x} + \frac{\partial M_y}{\partial y} + Q_y = 0$$

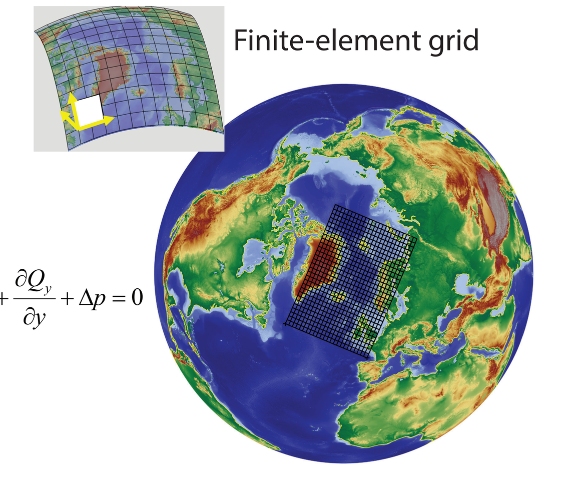

Finite-element grid

Geoid data (Pavlis et al., 2012) filtered so that only wave lengths within corresponding range contribute. The method, introduced by Coblentz et al. (2015) following Chase et al. (2002), assumes that "the upper mantle geoid" anomalies can be extracted by filtering, and these can be directly linked to GPE (x 2.3e11 N/m).

5.2 METHOD 3. GPE BASED ON LITHOSPHERIC DENSITY MODEL

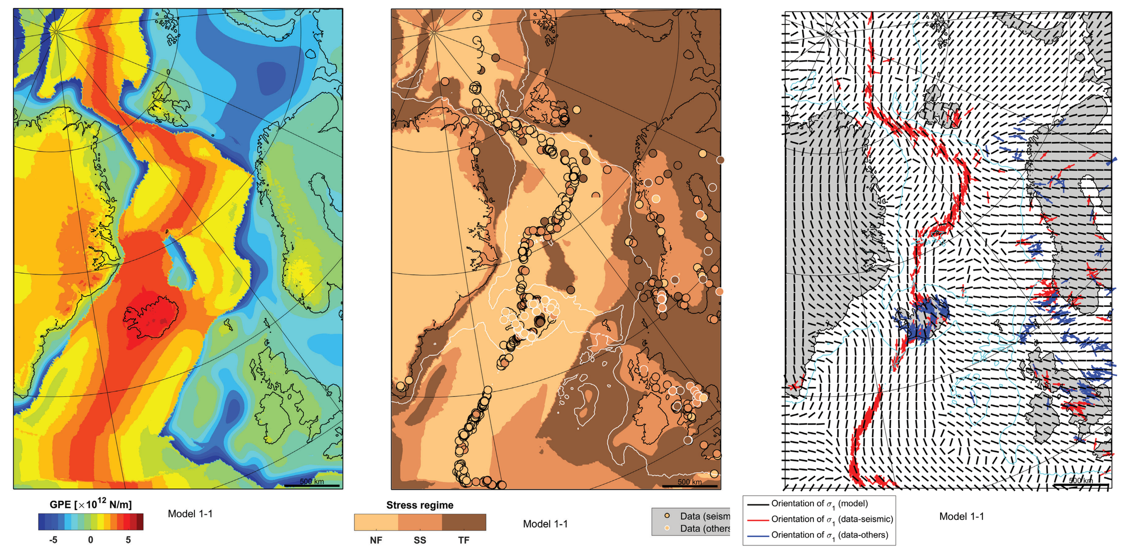

$$\Pi = \Pi_m + \Pi_c = g\Delta\rho_m\kappa t + \int_M^{S_{model}}\int_z^{S_{model}} \rho_c(x,y,z')g\,dz'\,dz$$

The total GPE estimated based on the lithospheric density model consists of mantle and crustal parts, respectively. The mantle part is derived based on the half-space cooling model. The mantle temperature is locally adjusted assuming that the observed large-scale (>300 km wavelength) topography is in isostatic equilibrium.

6. CONCLUSIONS

Our study presents the technique to adopt data, constrain models, and compare results between models and with observations. Although, the project is in the initial state and more thorough investigations are needed, we can bring some initial conclusions. All three methods predicts an extension regime in the area surrounding the mid-Atlantic ridge (MAR), Iceland, eastern Greenland and, locally, in SW Norway and parts of British Isles (extension+strike-slip regime). This regime is associated with a high gravitational potential and high radial gravity gradient values. Local compressive regime develops in the central Barents Sea, mid-Norwegian margin and North Sea. General stress regime and stress orientations in WSM data are captured by all three methods. We link these observations to lithospheric buldging and asthenospheric flow away from the Iceland hotspot.

References

Bouman, J. et al., 2016. Satellite gravity gradient grids for geophysics. Scientific reports 6.
Camelbeeck, T. et al., 2013. Local stress sources in Western Europe lithosphere from geoid anomalies. Lithosphere 5, 235-46.
Chase, C. et al., 2002. Colorado Plateau: Geoid and means of isostatic support. Int Geol Rev 44, 575-87.
Coblentz, D. et al., 2015. The upper mantle geoid: Implications for continental structure and the intraplate stress field. Geological Society of America Special Papers 514, 197–214.
Dahlen, F. A., Tromp, J., 1998. Theoretical global seismology. Princeton, p. 1025.
Delvaux, D. et al., 1997. Paleostress reconstructions and geodynamics of the Baikal region. Tectonophys.
Gaina, C. et al., 2017. Break-up and seafloor spreading domains in the NE Atlantic. Geol Soc London Spec Pub 447, SP447. 12.
Heidbach, O. et al., 2016. New Crustal Stress Map of the Mediterranean and Central Europe.
Medvedev, S., 2016. Understanding lithospheric stresses: systematic analysis of controlling mechanisms with applications to the African Plate. Geophys J Int 207, 393-413.
Pavlis, N.K. et al., 2012. The development and evaluation of the Earth Gravitational Model 2008 (EGM2008). J Geophys Res 117.
Schaeffer, A.J., Lebedev, S., 2013. Global shear-speed structure of the upper mantle and transition zone. Geophys J Int, ggt095.

Acknowledgements

The work is funded by European Space Agency (ESA) project "3D Earth - Dynamic Living Planet" and the Norwegian Reseach Council through its center of excellent scheme.